Available on CMS information server

CMS NOTE 2001/033

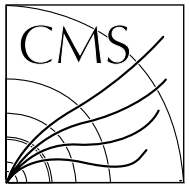

The Compact Muon Solenoid Experiment

CMS Note

Mailing address: CMS CERN, CH-1211 GENEVA 23, Switzerland

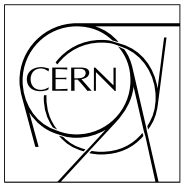

21 June 2001

Simulated Performance of the CSC Track-Finder

D. Acosta, M. Stoutimore, S.M. Wang

University of Florida, Gainesville, USA

Abstract

An object-oriented software description of the CSC Track-Finder has been written to exactly mimic the behavior of current prototypes. Using this package, the performance of the trigger has been simulated within the ORCA simulation framework to determine the transverse momentum resolution, trigger efficiency, and trigger rate. Degradation of the performance due to pile-up of minimum-bias collisions and neutron hits is also studied.

1 Introduction

The performance of the Cathode Strip Chamber (CSC) Track-Finder [1] for the Level-1 Muon Trigger has been simulated using the Object-oriented Reconstruction for CMS Analysis (ORCA) framework. A description of the CSC Track-Finder was written in C++ to exactly mimic the functionality of currently constructed prototypes. In fact, this code has been used to validate the hardware, where perfect agreement has been achieved between the electronic hardware and the software model for millions of events (random data and ORCA data). The results obtained from the ORCA simulation include the the transverse momentum resolution, trigger efficiency, and trigger rate, including the effects of pile-up backgrounds.

The endcap muon system of CMS consists of four stations (ME1–ME4) of CSC chambers on each end of the experiment, covering the range in pseudorapidity from 0.9 to 2.4 (see Fig. 1). A single station is composed of six layers of CSC chambers, where a single layer has cathode strips aligned radially and anode wires aligned in the orthogonal direction. The CSC chambers are trapezoidal in shape with either a 10° or 20° angular extent in azimuth (ϕ). The simulation of the response of the CSC chambers in ORCA, including the modeling of the front-end amplifier response, cross-talk, and noise, is described in Ref. [3]. At present, the performance of the cathode strip comparators in this simulation is naive, and a more realistic simulation may degrade the performance of the Level-1 Trigger.

The purpose of the CSC Track-Finder is to link trigger primitives (track segments) from individual CSC stations into complete tracks, measure the transverse momentum $p_{\rm T}$ from the sagitta induced by the magnetic bending, and report the number and quality of tracks to the Level-1 Global Muon Trigger. This objective is complicated by the non-uniform magnetic field in the CMS endcap and by the high background rates; consequently, the present design incorporates full three-dimensional information into the track-finding and measurement procedures.

A separate Track-Finder handles data from the barrel drift-tube system (see Ref. [4] for its simulation), and issues related to the overlap of the two systems is described in Ref. [5]. In particular, the boundary between the two systems is presently set at $\eta = 1.04$, although information is shared across this boundary to improve efficiency.

The first simulation results of the CSC Track-Finder were published in the Level-1 Trigger TDR [2] using ORCA release 4_3_2 and CMSIM version 118 (for the GEANT3 hit generation). It was shown that satisfactory rate reduction and efficiency could be achieved in the CMS Endcap Muon system at the design luminosity of $\mathcal{L} = 10^{34}$ cm^{-2}s^{-1}. The same simulation was used in an initial study of the Level-2 Trigger performance [6] as well. In the present study, improvements have been made to the $p_{\rm T}$ resolution of the Track-Finder, and the effect of backgrounds on the trigger performance are studied for the first time. Most results are obtained using CMSIM version 121[1)] (which uses an updated 3-D magnetic field map compared to the earlier studies) and ORCA release 4_5_1 (with the `L1CSCTrigger` and `L1CSCTrackFinder` packages updated to that of 4/26/01). Details of the datasets used in the simulation will be given in the relevant sections.

2 Level-1 CSC Trigger Architecture

The architecture of the Level-1 CSC Trigger is described in detail in Ref. [2], and is illustrated by the block diagram in Fig. 2. A Local Charged Track (LCT) forms the most primitive trigger object of the endcap muon system. Both cathode and anode front-end LCT trigger cards search for valid patterns from the six wire and strip planes of a CSC station. The anode data provide precise timing information as well as η information, and the cathode data provide precise ϕ information. Comparators on the cathode cards localize a hit cluster to within a half-strip for each layer. A Trigger Motherboard collects the LCT information from one chamber, associates the wire data to the cathode data, tags the bunch crossing time, and selects the two best candidates.

The combined LCTs are funneled through Port Cards to reduce the bandwidth sent to the CSC Track-Finder. Each Port Card collects track segments from up to nine chambers (18 associated LCTs) and selects the three best candidates. A total of three (six) LCTs are forwarded from a 60° azimuthal sector in ME2–ME4 (ME1).

The track segments from the Port Cards are received by the CSC Track-Finder in Sector Receiver cards. The Sector Receiver cards receive the LCTs from all four stations in one 60° sector, reformat the track segments into global coordinates suitable for the track-finding algorithms, and apply alignment corrections to the data to account for placement errors of the CSC chambers. The track-finding algorithms that identify muons from this data are implemented in 12 Sector Processor cards (described below), and the output of each Sector Processor is the momentum and quality of the three best muon candidates found in each 60° sector.

[1)] A bug fix to the routine `mc_junk.F` was included to correct a problem in the neutron background simulation.

The final stage of the Level-1 CSC Trigger is the CSC Muon Sorter, which collects the output of all Sector Processors and selects the four highest-rank muons from the entire CMS endcap muon system (a total input of up to 36 muons). The output of the Muon Sorter is sent to the Global Muon Trigger, which associates barrel and endcap muon candidates with RPC muon candidates and with quiet regions in the calorimeter. The best 4 muons of CMS are then sent to the Global Level-1 Trigger, where specific p_{T} thresholds are applied to the muon candidates.

The simulation of the CSC trigger primitive generation, including the Sector Receiver, is the subject of Ref. [7]. The simulation of the trigger processing of the Sector Processor, which performs the regional track-finding in 60° sectors, is the subject of this Note. The simulation of the Global Muon Trigger, which combines the DT, CSC and RPC muon systems, is described in Ref. [8].

3 Track-Finding Logic

The CSC Sector Processor reconstructs tracks from the track segments delivered by the Sector Receivers and the DT Track-Finder in one 60° azimuthal region. The number of CSC track segments collected by one Sector Processor is 15 per bunch crossing. Six track segments are delivered from ME1, and three each are delivered from ME2–ME4. Additionally, four DT track segments are delivered from the MB1 chambers in the outer wheel of the barrel muon system.

The track-finding logic implemented in the current Sector Processor prototype is described in detail in Refs. [1, 2]. Briefly, the reconstruction of complete tracks from individual track segments is partitioned into several steps. First, the track segments from the CSC and DT trigger systems must be synchronized and possibly held for more than one bunch crossing to accommodate bunch-crossing misidentification. The selection logic that chooses which track segments to use at a given bunch crossing is referred to as the "Bunch Crossing Analyzer." Next, nearly all possible pairwise combinations of track segments are tested for consistency with a single track in various "Extrapolation Units" (one for each pair of stations). That is, each track segment is extrapolated to another station and then compared to the spatial information of other track segments in that station. Successful extrapolations yield tracks composed of two segments, which is the minimum necessary to form a trigger. If an ambiguity is created when two muons enter the same CSC chamber (ghost hits), all possible η–ϕ combinations are tried (ME1 only). A direct approach to resolve the ghost combinations at the chamber level has been proposed [9] as well using information from the Resistive Plate Chamber (RPC) muon detection system.

A muon which traverses all four muon stations yields six combinations of station pairs (although only five are considered by the Sector Processor); thus, the next step is to assemble complete tracks from the extrapolation results and cancel redundant shorter tracks. There are three of these "Track Assembler Units"—one for tracks with a segment in ME2, one for tracks with a segment in ME3, and one for tracks in ME2 in the DT/CSC overlap region. The results are sorted and redundant tracks cancelled in the "Final Selection Unit," which selects up to the three best *distinct* tracks. Finally, the momenta of these candidates are measured in the "Assignment Unit."

The overall scheme for the Sector Processor is illustrated in Fig. 3. In the ORCA software package, most subprocessors (the Extrapolation Unit, Track Assembler Unit, Final Selection Unit, and Track Assignment Unit) are implemented as a class contained by the principal Sector Processor class. Separate classes encapsulate the data exchanged between the subprocessors. The functionality of the classes emulates the hardware bit-for-bit.

It should be noted that in the current simulation, the Bunch Crossing Analyzer of the Sector Processor is not implemented. This means that only in-time trigger primitives are considered from both the CSC and DT systems, whereas it is foreseen to allow at least one segment of a track to be out-of-time in the final trigger hardware to improve efficiency. Additionally, the track segment quality and bend angle ϕ_b are not yet used in the Extrapolation Units. A separates study needs to be performed to determine how to best use this information to reject backgrounds and maintain good muon efficiency.

Finally, we have studied the effect of doubling the size of the p_{T} assignment look-up memory from what was originally proposed in Ref. [1] to accommodate 1-bit of z-information. Since the CSC chambers are staggered in z for a given disk (so that they overlap), labeling whether the chamber is closer or farther from the interaction point improves the p_{T} resolution.

4 Momentum Assignment

The most important factor that governs the efficiency and rate of the Level-1 CSC Trigger is the resolution of p_{T}. A poor resolution means that some signal muons will fluctuate below the trigger threshold, causing a loss

of efficiency, and some low momentum muons from minimum bias collisions will fluctuate above the trigger threshold, causing high rates. The p_{T} assignment of the CSC Track-Finder was first explored in Ref. [10] using CMSIM, and a resolution of about 20% is necessary to have sufficient background rejection.

The Track Assignment Unit of the Sector Processor performs the measurement of the transverse momentum and other track parameters for all identified muons. This is accomplished using an FPGA for preprocessing followed by a large look-up memory for the final calculation. The output includes a 5-bit p_{T} word, a 2-bit quality (taken to mean the uncertainty in the measurement), a muon sign bit, and η and ϕ coordinates (reported at the position of ME2). The p_{T} and quality are encoded into a 7-bit rank for sorting in the CSC Muon Sorter. The p_{T} scale is programmable, but is chosen to be the nonlinear scale proposed in Ref. [2] and listed in Tab. 1. The quality word is defined in Tab. 2. A quality code of 3 denotes a track with the best p_{T} measurement possible. A quality code of 1 denotes a track where the measurement of the p_{T} is very uncertain, if known at all. In fact, all such low quality tracks in the DT/CSC overlap region have the p_{T} word arbitrarily set to the maximum to maintain high efficiency (at the expense of trigger rate) because the p_{T} resolution is so poor without a segment in MB1. Likewise, the muon sign is fixed at either positive or negative.

Analytic expressions have been derived to estimate the track momentum from the sagitta induced by the magnetic field. This maintains generality so that the method is not tied to the exact hardware implementation of the p_{T} assignment. For example, the p_{T} scale may change, the precision of the track segment data might change, or the binning of η and ϕ coordinates could change. The exact contents of the Track-Finder look-up memories are derived from these analytic expressions.

4.1 Method of Parameterization

4.1.1 Two-Station Assignment

The simplest method to measure the transverse momentum is to exploit the inverse relationship between p_{T} and the ϕ difference between track segments in two stations: $p_{\mathrm{T}} = a/\Delta\phi$. However, because the magnetic field is nonuniform in the CMS endcap, and because the amount of bending depends on which two stations are involved, the expression used is:

$$p_{\mathrm{T}} = \frac{A_{ij}(\eta)}{\Delta\phi_{ij}} \tag{1}$$

where $A_{ij}(\eta)$ is a function that varies with pseudorapidity, and i and j label which two stations are involved. A more accurate expression that handles deviations from this inverse relationship at low momentum is based on:

$$\Delta\phi_{ij} = \frac{A(\eta)}{p_{\mathrm{T}}} + \frac{B(\eta)}{p_{\mathrm{T}}^2} \tag{2}$$

where p_{T} is obtained by solving the quadratic equation. Third-order polynomials have been fit to the results of CMSIM and ORCA in order to determine $A(\eta)$ and $B(\eta)$ for both two-station methods. A slight difference in the fits ($\sim 10\%$) is observed between CMSIM version 118 (which uses the older $2D$ B-field parameterization) and 121 (which uses the newer $3D$ parameterization) in the region $1.0 < |\eta| < 1.6$.

4.1.2 Three-Station Assignment

The accuracy of the p_{T} assignment improves when more of the muon trajectory is used in the fit. In particular, it was found in Ref. [10] that the p_{T} resolution improves at low momentum to about 20% when track segment data from three stations are used (of which one segment must come from ME1). The Track-Finder hardware has been designed to perform such a three-station measurement using the ϕ difference between the first and second station ($\Delta\phi_{12}$), the ϕ difference between the second and third station ($\Delta\phi_{23}$), η, and a 4-bit flag specifying which stations are involved. Although the average $\Delta\phi_{23}$ is small compared to $\Delta\phi_{12}$ because of the reduced magnetic flux, fluctuations in $\Delta\phi_{23}$ are large at low momentum because of multiple scattering. Hence, the overall p_{T} resolution improves.

An estimator of the transverse momentum has been derived from the method of maximum likelihood (although it is equivalent to a Chi-square minimization since we assume that $\Delta\phi$ is Gaussian distributed). Correlation between $\Delta\phi_{12}$ and $\Delta\phi_{23}$ is included. This leads us to consider a bivariate normal distribution for the likelihood function:

$$\mathcal{L} = \frac{1}{2\pi\sigma_{12}\sigma_{23}\sqrt{1-\rho^2}} \times \exp\left\{\frac{-1}{2(1-\rho^2)}\left[\frac{(\Delta\phi_{12}-\mu_{12})^2}{\sigma_{12}^2} - \frac{2\rho(\Delta\phi_{12}-\mu_{12})(\Delta\phi_{23}-\mu_{23})}{\sigma_{12}\sigma_{23}} + \frac{(\Delta\phi_{23}-\mu_{23})^2}{\sigma_{23}^2}\right]\right\} \quad (3)$$

where μ_{ij} is a function taken from the two-station $p_{\rm T}$ assignment, $\mu_{ij} = A_{ij}(\eta)/p_{\rm T}$, σ_{ij} is the spread in $\Delta\phi_{ij}$, and ρ is the correlation coefficient between $\Delta\phi_{12}$ and $\Delta\phi_{23}$. The resolution $c_{ij} \equiv \sigma_{ij}/\mu_{ij}$ is assumed to be independent of $p_{\rm T}$ (which is a good approximation at low momentum where multiple scattering dominates over the position resolution). The correlation coefficient has been found to be approximately 0.6.

An estimate of the transverse momentum is obtained by maximizing the likelihood. This can be done analytically by setting $d\mathcal{L}/dp_{\rm T} = 0$ and solving for $p_{\rm T}$ (the details can be found in Ref. [11]). Note that no explicit fit of the three-station formula to simulation data is performed. Only the two-station functions $A_{ij}(\eta)$ and $c_{ij}(\eta)$ are fit. The result is a reasonable parameterization of the correlated behavior of $\Delta\phi_{23}$ versus $\Delta\phi_{12}$ as a function of $p_{\rm T}$, as can be seen from Fig. 4 for the region $2.0 < |\eta| < 2.1$. The scatter plot shows simulated data for $p_{\rm T} = 3$, 5, and 10 GeV/c, and the contours are the result of the three-station parameterization for the same fixed values.

The 3-station $p_{\rm T}$ measurement yields superior resolution over the 2-station measurement only when the bending between the second and third stations, $\Delta\phi_{23}$, is significantly larger than the precision of the measurement. Thus, if the precision of $\Delta\phi_{23}$ is made finer, the range of $p_{\rm T}$ over which the $p_{\rm T}$ resolution will be improved increases. In the current ORCA_4_5_1 trigger primitive simulation, the precision of ϕ (its effective binning) is limited to 1/2 of a CSC strip (≈ 2.3 mrad for a 20° chamber at high η) since the LCT pattern type is not yet considered in the determination. This limits the improvement in the $p_{\rm T}$ resolution over the 2-station method to approximately $p_{\rm T} < 10$ GeV/c, and the current Track-Finder simulation in ORCA switches between the 3-station and 2-station method when $\Delta\phi_{23} < 4$ mrad.[2)] The ultimate ϕ precision should be better than 2.3 mrad, however, as a given CSC chamber has 6 layers of measurements at this precision. The ultimate resolution is expected to be $2.3\ \text{mrad}/\sqrt{6\times 12} = 0.27$ mrad, which justifies the use of 12 bits of ϕ in the hardware for a 60° azimuthal trigger sector.

4.2 $p_{\rm T}$ Resolution

Figure 5 shows the residual distribution of $(1/p_{\rm T}^{\rm meas} - 1/p_{\rm T}^{\rm true})/(1/p_{\rm T}^{\rm true})$ for reconstructed tracks with segments in at least two CSC stations, of which one must be ME1. The muons were generated with a flat distribution over the intervals $5 < p_{\rm T}^{\rm true} < 35$ GeV/c and $1.2 < |\eta| < 2.0$. The reconstructed $p_{\rm T}^{\rm meas}$ uses the non-linear scale listed in Tab. 1, and the measurement is reported at 50% efficiency (*i.e.* the residual distribution should have a mean of zero). The top plot shows the residual distribution for the $p_{\rm T}$ assignment method used at the time of Level-1 TDR publication [2] in ORCA_4_3_2. The bottom plot shows the improvement in the $p_{\rm T}$ resolution when the staggering of the ME1 chambers is taken into account, as included in the latest release of the `L1CSCTrigger` and `L1CSCTrackFinder` packages. Since most of the magnetic return flux occurs close to the ME1 chambers, the amount of bending between ME1 and ME2 varies by 25% depending on whether the ME1 chamber is closer or farther from the interaction point. With a Gaussian fit to the central 2σ of the distribution, the resolution improves from 26% to 22% taking this variation into account. This 1-bit of z information will be added to the $p_{\rm T}$ assignment hardware of the CSC Track-Finder.

Figure 6 shows the $p_{\rm T}$ resolution as a function of η for several generated $p_{\rm T}$ values. Reconstructed tracks are required to have segments in at least two CSC stations, including one in ME1, and the stagger of the ME1 chambers is taken into account. The current LCT trigger simulation is used with its limited 1/2-strip ϕ precision. The resolution is determined from a Gaussian fit to the central 2σ of the residual distribution. The best resolution is achieved for $p_{\rm T} = 10$ GeV/c, where it is better than 20% over most of the η coverage. The resolution degrades for lower and higher momenta. If the reconstructed tracks did not have a segment in ME1 (or MB1 in the DT/CSC overlap), the resolution would be considerably worse ($> 70\%$, see Ref. [10]).

[2)] We have to allow a separation of two ϕ bins from zero so that muons on a 1/2 strip boundary are not given an artificial bend, which would significantly worsen the 3-station $p_{\rm T}$ resolution.

5 Track-Finding Efficiency

The CSC trigger efficiency, as estimated from ORCA_4_5_1, for single muons as a function of η is shown in Fig. 7 for two sets of criteria applied to tracks found by the CSC Track-Finder. Figure 7a illustrates the case when ME4 participates in the trigger, and Fig. 7b illustrates the case when it is removed. The solid line in each figure shows the efficiency for tracks that have segments in at least two muon stations, of which one must be ME1 for the endcap region ($|\eta| > 1.2$) in order to maintain satisfactory p_{T} resolution. Any two stations are allowed for the DT/CSC overlap region ($1.05 < |\eta| < 1.2$) to keep the efficiency high[3] In contrast to this loose set of conditions, the dashed line in each figure shows the efficiency for tracks when segments in at least three muon stations are required, including one from ME1 in the endcap region and one from MB1 in the DT/CSC overlap, so that the best p_{T} resolution is achieved. The efficiency is reduced in this case, particularly in the DT/CSC overlap as well as for the case when only 3 CSC stations are present, because of a lack of redundancy. However, the background rejection will be a maximum. The configuration used in the trigger is a trade-off between efficiency and increased rate from low quality tracks. At high luminosity, we expect that three stations will be required if the CSC system is used standalone, without coincidence with the RPC system.

The CSC trigger efficiency for single muons as a function of ϕ is shown in Fig. 8 for the case when ME4 is included. The solid line corresponds to the loose set of track requirements just described, and the dashed line corresponds to the tighter set. The overall CSC trigger efficiency is 92.5% for muons generated in the range $1.05 < |\eta| < 2.4$ using the loose set of criteria, and is flat in ϕ. For the tight track criteria, the efficiency drops to 74% because of the geometric holes in the η coverage seen in Fig. 7. If the station ME4 is removed, the efficiency for the loose track criteria remains the same,[4] whereas the efficiency for the tight track criteria drops to 67.5%.

Figure 9 shows the trigger efficiency turn-on curves as a function of the true p_{T} for several trigger thresholds (defined at 90% of the maximum efficiency) for the loose set of track criteria in the endcap region. The sample of single muons used for the study are generated flat in pseudorapidity, $1.2 < |\eta| < 2.4$, so the p_{T} resolution is an average over this interval. The curves are fits to the theoretical expectation of the shape assuming that $1/p_{\mathrm{T}}$ is Gaussian distributed:

$$\varepsilon(p_{\mathrm{T}}) = \frac{1}{2}\mathrm{erf}\left(\frac{p_{\mathrm{T}}/p_{\mathrm{T}}^{50}+1}{\sqrt{2}c}\right) + \frac{1}{2}\mathrm{erf}\left(\frac{p_{\mathrm{T}}/p_{\mathrm{T}}^{50}-1}{\sqrt{2}c}\right) \tag{4}$$

Here the two fit parameters are p_{T}^{50}, which is the trigger threshold defined at 50% efficiency (the 90% efficiency threshold is about 40% larger), and c, which is the p_{T} resolution (assumed a constant percentage of p_{T}). From the fits, the average resolution is about 30% over this interval. The above equation is multiplied by a first-order polynomial to parameterize the slope in the efficiency at high p_{T}.

The tendency of the trigger efficiency to decrease slightly at high p_{T} is caused by electromagnetic radiation (bremsstrahlung and e^+e^- pair-production) from the high momentum muon. This can be inferred from Fig. 10, which shows the same trigger efficiency curves for multiple-scattering only. In this case, the trigger efficiency remains a constant 90% as a function of p_{T}. The difference amounts to about 4% at $p_{\mathrm{T}} = 100$ GeV/c. For a muon with $p_{\mathrm{T}} = 300$ GeV/c (momentum of order 1 TeV/c), the trigger efficiency drops to 82%. The presence of the shower products disturbs the timing and pattern recognition logic of the LCT trigger, particularly when secondary clusters arise which are separated from that of the muon.

The trigger efficiency also decreases when pile-up backgrounds from minimum-bias collisions are superimposed, as extra hits will degrade the position resolution. Figure 11 shows the degradation of the single muon efficiency as a function of p_{T} for a trigger threshold of 20 GeV/c. The track conditions are the same as for Fig. 9 (ME4 included), but with the background conditions simulated for a luminosity of 0, 10^{34}, and 3×10^{34} cm^{-2}s^{-1}. Specifically, 17.3 minimum-bias collisions are piled-up in the current beam crossing for $\mathcal{L} = 10^{34}$ cm^{-2}s^{-1}. Pile-up from out-of-time beam crossings is not presently considered, except that the neutron induced background from much earlier crossings is included using the parameterization available in CMSIM for the appropriate luminosity. The overall trigger efficiency drops about 3%, independent of p_{T}, when backgrounds corresponding to a luminosity of 10^{34} cm^{-2}s^{-1} are included. The drop is 10% when the luminosity is three times higher. It is the neutron background that affects the efficiency most.

[3] The efficiency in the DT/CSC overlap region is explored in more detail in Ref. [5].

[4] This is because the present Sector Processor design requires a track segment in ME2 or ME3.

6 Trigger Rate

The CSC single muon trigger rate is estimated from simulated samples of minimum bias events. At an LHC luminosity of 10^{34} cm^{-2}s^{-1}, an inelastic cross section of 55 mb corresponds to an average of 17.3 minimum bias collisions every beam crossing (assuming that 80% of the beam buckets are filled). It is generally assumed that most of the single muon trigger rate comes from real muons from prompt c and b-quark decays as well as non-prompt π and K decays.

The Level-1 trigger rates included in the Level-1 TDR [2] were estimated using Monte Carlo samples described in more detail in Ref. [12]. In particular, the PYTHIA 6 generator was used to generate samples of minimum bias collisions, and an interface was added to force at least one particle in an event to decay to a muon and to generate a weight for that event. These weighted event samples (which are significantly smaller in size than the corresponding unweighted sample) were then passed through CMSIM version 118 for the hit generation, combined with pile-up, and digitized in ORCA release 4_3_2.

Figure 12 shows the single muon trigger rate from the CSC trigger obtained using these weighted event samples as a function of the p_{T} threshold applied (defined at 90% efficiency according to the binning shown in Tab. 1). The solid line corresponds to the loose set of criteria described in Sec. 5, which yields good trigger efficiency but high rate (> 10 kHz for any threshold). This rate can be reduced to acceptable levels by the Global Muon Trigger, however, when the CSC tracks are combined with RPC tracks, as discussed in Ref. [8]. On the other hand, the CSC trigger alone can reduce the rate to acceptable levels when the requirement on the tracks reported by the CSC Track-Finder is tightened, as shown by the dashed line in Fig. 12. A single muon rate of about 5 kHz is achieved when the single muon threshold is set to 25 GeV/c because of the improved p_{T} resolution of high quality tracks, at the expense of 20% efficiency loss.

The weighted minimum bias results are potentially biased because they do not include triggers arising from punch-through or other random coincidences. Each event is forced to include a muon. Thus, to study the absolute trigger rate, a sample of 130,000 unbiased minimum bias events was created using PYTHIA 6, CMSIM version 121, and ORCA release 4_5_1. Additionally, a sample of "signal" events containing only neutron hits from the latest neutron background parameterization was generated. The minimum bias sample can be analyzed one collision at a time (without the effects of pile-up) or combined with a Poisson average 17.3 collisions per beam crossing with the neutron background sample. Only in-time pile-up of the minimum bias sample is considered. The resulting trigger rate is shown in Fig. 13. The dashed curves include the effects of pile-up and the neutron background, the solid curves do not. The upper two curves are for loose track requirements, while the lower two curves are for tight requirements. The overall trigger rate is about 30% larger than the rate obtained using the weighted minimum bias samples. The estimated trigger rate differs by less than 5% when pile-up and neutrons are included. This decrease is consistent with the 3% drop in trigger efficiency when the neutron background is included, confirming that most of the rate comes from real muons rather than random coincidences.

Figure 14 shows the trigger rate with and without the presence of ME4 participating in the trigger. The rate corresponding to the loose set of track criteria is approximately 50% larger at high p_{T} when ME4 is excluded. The reason for this is that there are fewer 3-station tracks reconstructed, and this implies that the p_{T} resolution will be worse. On the other hand, almost no change is seen in the trigger rate for the tight set of conditions because all tracks are required to be 3 stations in length.

Finally, the trigger rate as a function of η is shown in Fig. 15 for two p_{T} thresholds: 0 and 10 GeV/c. The loose track criteria are applied. It can be seen that the DT/CSC overlap region ($|\eta| < 1.2$) contributes a larger percentage of the rate at higher p_{T}.

In all cases, the trigger rate was determined over the interval $1.05 < |\eta| < 2.4$. A reduction factor of 1.5–2.0 is possible if the very forward region $|\eta| > 2.1$ is excluded. This corresponds to the inner portion of the ME 1/1 chambers, and this region has poor p_{T} resolution due to the limited magnetic bending in the forward region.

7 Limitations and Conclusions

What is still lacking in the current simulation is the modeling of the Bunch Crossing Analyzer of the Sector Processor, which sorts and selects trigger primitives from out-of-time bunch crossings, and additional cuts based on the track segment quality and bend angle that could be applied in the Extrapolation Units to reduce backgrounds. The Track Assignment Unit also could be modified to use the bend angle ϕ_b to improve the p_{T} resolution when only two track segments are found (or in lieu of the third track segment should that provide better resolution). However, improvements to the CSC local trigger software must be made to calculate the bend angle (though it is

foreseen to be implemented in the hardware). The bend angle from DT track segments is already available in the ORCA software. Finally, the ϕ resolution of the CSC local trigger may improve when more information from the chamber pattern is used, and this could improve the p_{T} resolution from what is reported here. On the other hand, this may be offset by a more realistic modeling of the noise for the cathode strip comparators.

Acknowledgements

We would like to thank T. McDonald for his assistance with the p_{T} parameterizations as part of his NSF-sponsored REU project at the University of Florida. Also, we would like to thank A. Madorsky for his assistance in debugging not only the Sector Processor hardware, but the current software model as well.

Appendix A: User Settings

The switches that are available to the user to control the CSC Track-Finder simulation are listed in Tab. 3. The settings are applied in the `.orcarc` file, and are captured by the `L1MuCSCTrackFinderSetup` class in the `L1MuCSCTrackFinder` package.

References

[1] D. Acosta *et al.*, "The Track-Finding Processor for the Level-1 Trigger of the CMS Endcap Muon System," CMS NOTE-1999/060; D. Acosta *et al.*, "The Track-Finding Processor for the Level-1 Trigger of the CMS Endcap Muon System," Proceedings of the Fifth Workshop on Electronics for LHC Experiments, Snowmass, CERN/LHCC 1999-33.

[2] CMS, The TriDAS Project Technical Design Report, Volume 1, CERN/LHCC 2000-38

[3] T. Cox and R. Wilkinson, "Simulating the Muon Endcap," CMS NOTE-2001/013

[4] N. Neumeister, `http://neumeist.home.cern.ch/neumeist/trigger/mttf.html`

[5] M. Dallavalle *et al.*, "Issues related to the separation of the barrel and endcap muon trigger track-finders," CMS IN-1999/015; D. Acosta *et al.*, "Coverage of the DT/CSC Overlap Region by the Level-1 Track-Finders," CMS IN Note in preparation.

[6] D. Acosta *et al.*, "Results on L2 Trigger Reconstruction in Single and Di-Muon Topologies," CMS NOTE-2001/011.

[7] B. Tannenbaum, "Endcap Muon Trigger Primitive Software," CMS NOTE in preparation.

[8] H. Sakulin and M. Fierro, "Studies of the Global Muon Trigger Performance," CMS NOTE-2001/003.

[9] G.Wrochna *et al.*, "CMS Endcap Muon RPC–CSC Trigger Connection," CMS-IN 1998/030

[10] S.M. Wang and D. Acosta, "Simulation Studies on the Transverse Momentum Resolution of the CSC Track-Finder," CMS IN-2000/026.

[11] T. McDonald and D. Acosta, "Studies of the Optimum Momentum Resolution in the CMS Muon System," `http://www.phys.ufl.edu/REU/2000/reports/mcdonald/mcdonald.pdf`

[12] N. Neumeister *et al.*, "Monte Carlo simulation for High Level Trigger studies in single and di-muon topologies," CMS IN-2000/053.

Table 1: The 5-bit p_{T} scale used in the simulation. The floating point value refers to the low edge of the bin.

Bit Code	0	1	2	3	4	5	6	7	8	9
p_{T} (GeV/c)	–	0.	1.5	2.0	2.5	3.0	3.5	4.0	4.5	5.0
Bit Code	10	11	12	13	14	15	16	17	18	19
p_{T} (GeV/c)	6.0	7.0	8.0	10.	12.	14.	16.	18.	20.	25.
Bit Code	20	21	22	23	24	25	26	27	28	29
p_{T} (GeV/c)	30.	35.	40.	45.	50.	60.	70.	80.	90.	100.
Bit Code	30	31								
p_{T} (GeV/c)	120.	140.								

Table 2: Definition of the 2-bit quality code generated by the CSC Track-Finder.

Code	Meaning
0	no track
1	track in the DT/CSC overlap ($\|\eta\| < 1.2$) without a segment in MB1
1	track in the CSC region ($\|\eta\| > 1.2$) without a segment in ME1
2	two-station track with a segment in ME1 or MB1, or three-station tracks of the type ME1–ME3–ME4
3	three or four station track with a segment in ME1 or MB1, ME2, and ME3 or ME4

Table 3: Available settings to control the CSC Track-Finder simulation from the `.orcarc` file.

Flag	Default	Explanation
CSCTrackFinder:shareMB1	true	Control whether track segments from MB1 are used in the DT/CSC overlap
CSCTrackFinder:shareMB2	false	Control whether track segments from MB2 are used in the DT/CSC overlap
CSCTrackFinder:fourthStationConfig	3	Control whether no track segments from ME4 are allowed (0), ME4/1 only allowed (1), ME4/2 only allowed (2), or whether all of ME4 participates (3)
CSCTrackFinder:ghostBustME1	true	Control whether the ghost-busting feature is enabled for ME1 in the Extrapolation Unit

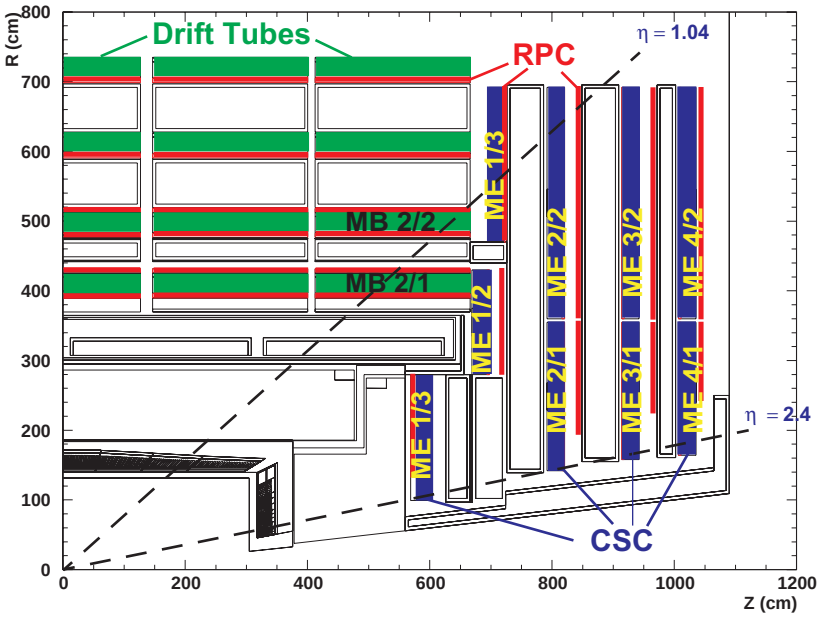

Figure 1: Illustration of the CMS muon system. The boundary at $\eta = 1.04$ divides the DT and CSC Track-Finders.

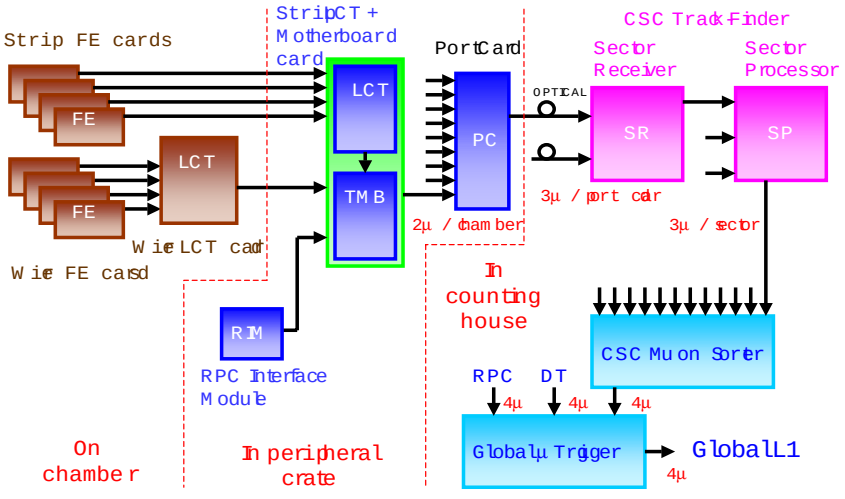

Figure 2: Architecture of the Level-1 CSC trigger.

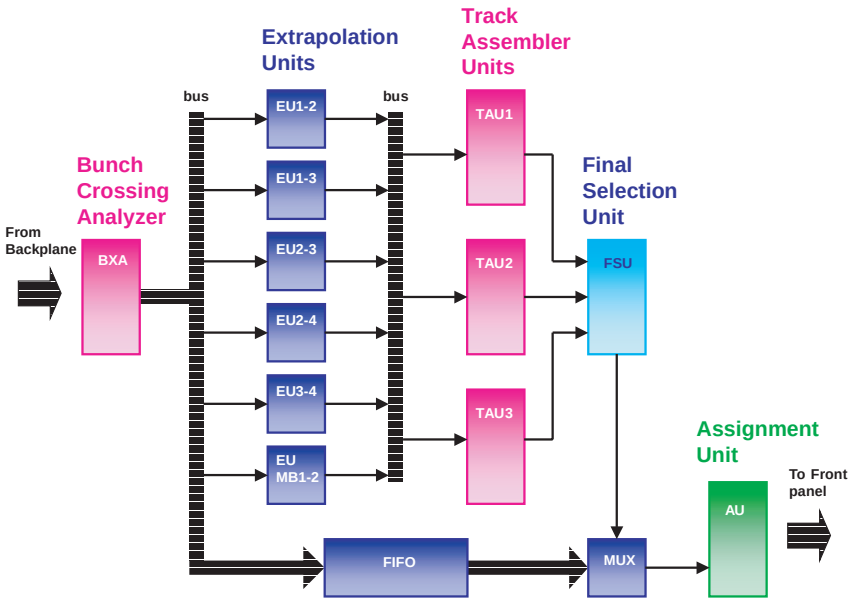

Figure 3: Block diagram of the Sector Processor logic.

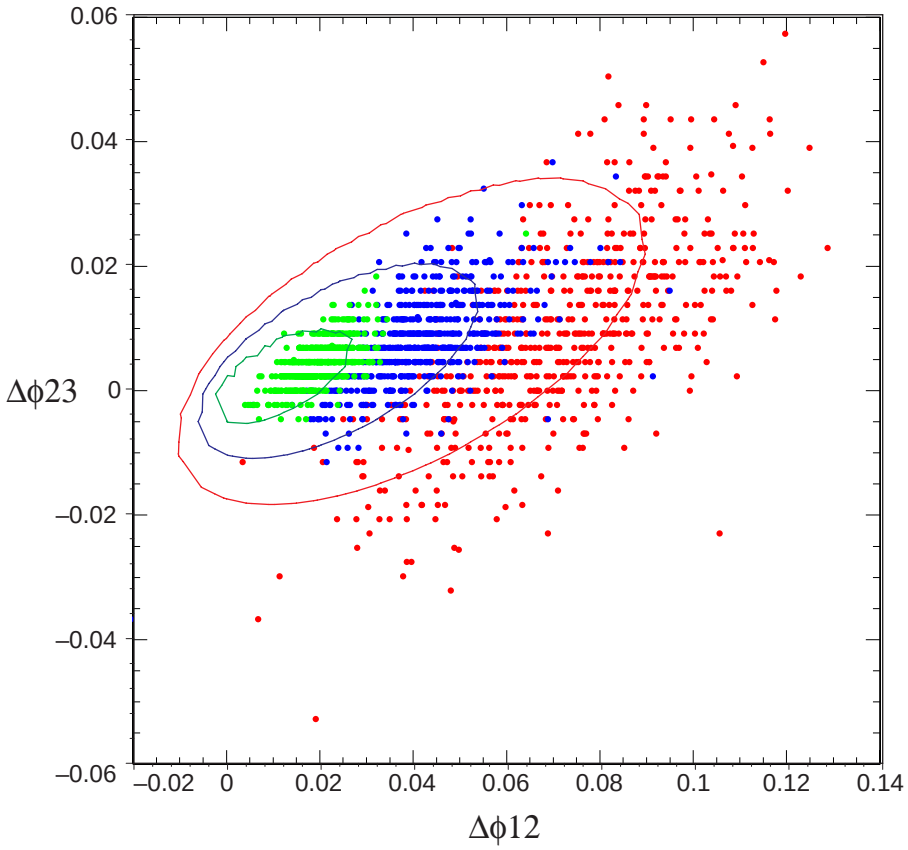

Figure 4: A scatter plot of $\Delta\phi_{23}$ versus $\Delta\phi_{12}$ in radians from CMSIM for $p_{\mathrm{T}} = 3$ GeV/c (red), 5 GeV/c (blue), and 10 GeV/c (green) in the region $2.0 < |\eta| < 2.1$. Overlaid are the results of the three-station parameterization for the same momenta.

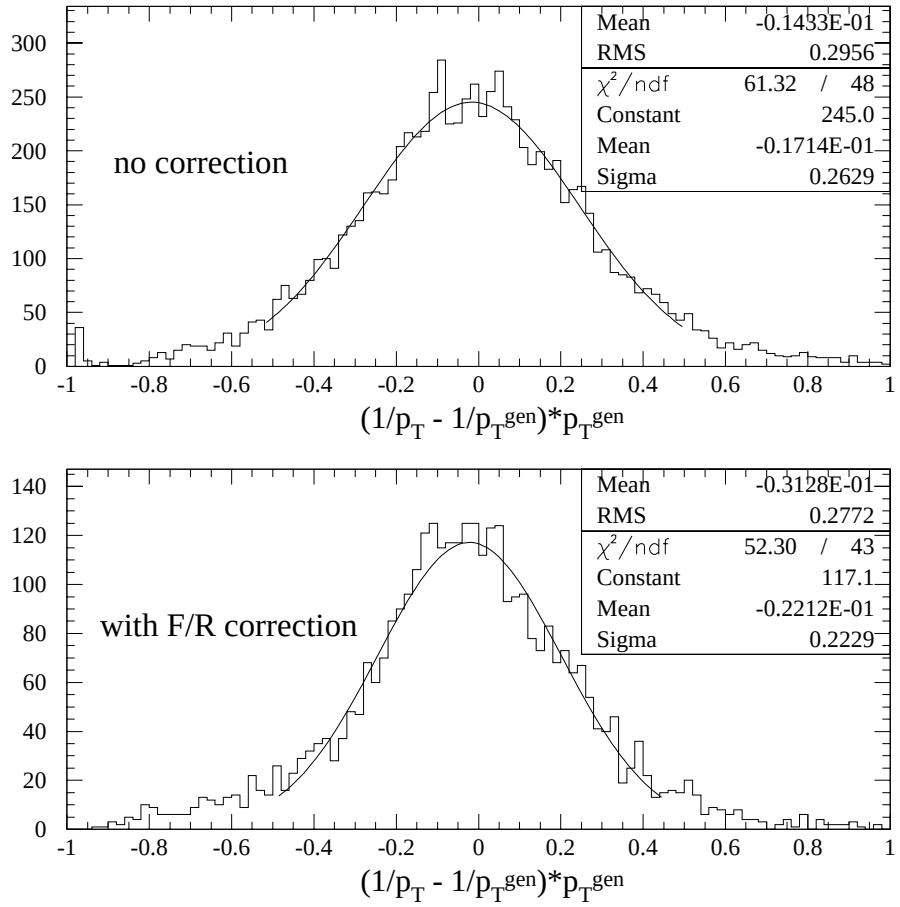

Figure 5: Residual distribution of the inverse transverse momentum measured by the CSC Track-Finder for single muon generated flat in $3 < p_{\mathrm{T}} < 35$ GeV/c and $1.2 < |\eta| < 2.0$. A track in ME1 is required. The top plot is without any correction to the ME1 stagger, while the bottom plot includes it.

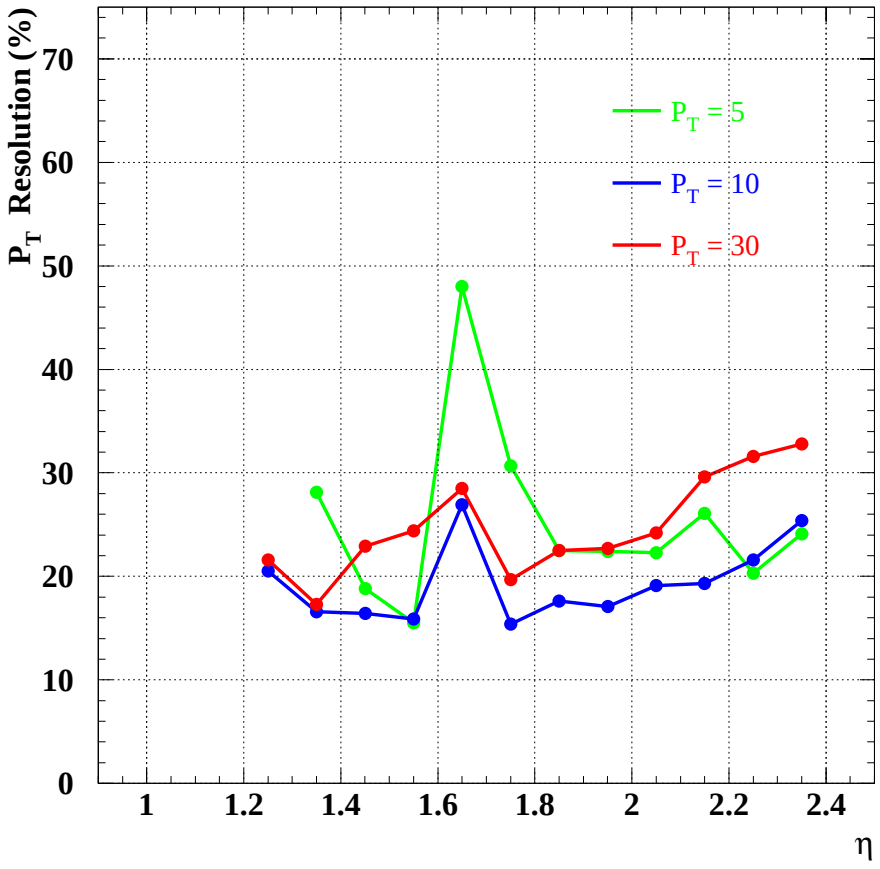

Figure 6: The p_{T} resolution of the CSC Track-Finder as a function of η for $p_{\mathrm{T}} = 5$, 10, and 30 GeV/c.

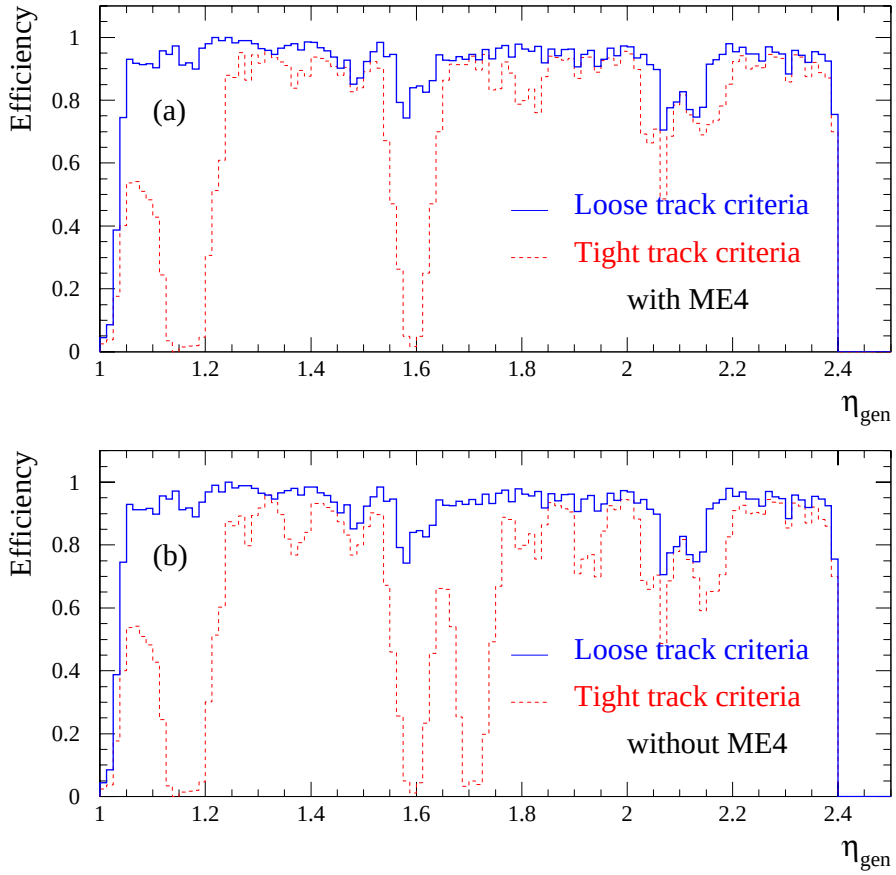

Figure 7: The CSC Track-Finder efficiency for single muons as a function of η, with (a) and without (b) ME4 in the trigger. The solid line corresponds to loose requirements on the track quality, the dashed line corresponds to tight requirements (see text).

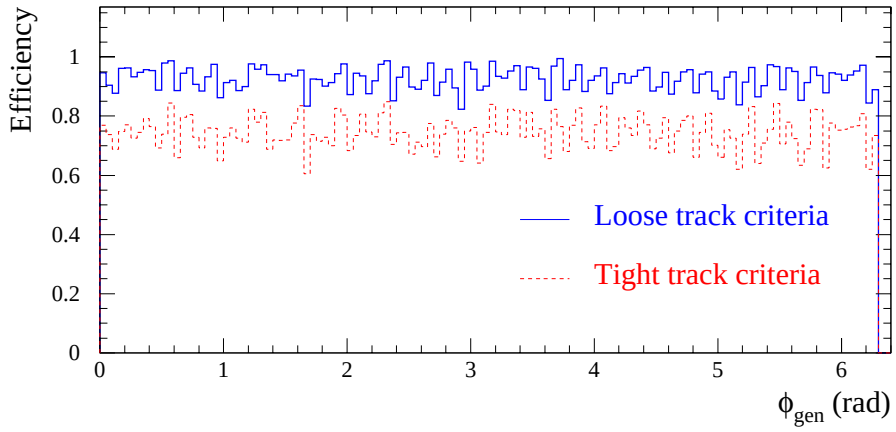

Figure 8: The CSC Track-Finder efficiency as a function of ϕ for single muons. The solid line corresponds to loose requirements on the track quality, the dashed line corresponds to tight requirements.

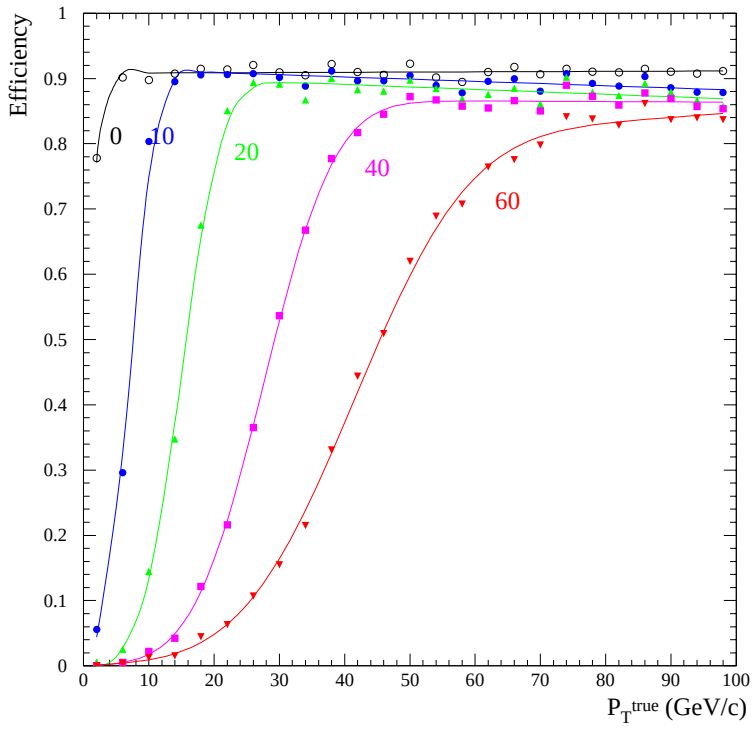

Figure 9: CSC trigger efficiency turn-on curves as function of the true p_{T} for several trigger thresholds. The p_{T} thresholds are defined at 90% efficiency.

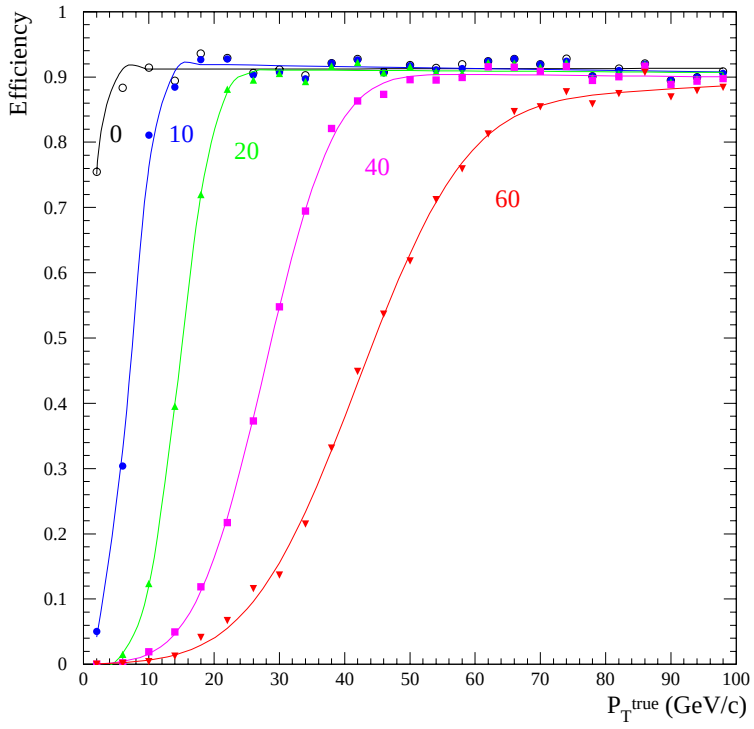

Figure 10: The same trigger efficiency curves as shown in Fig. 9, but with muon bremsstrahlung and pair-production turned off in the simulation (multiple scattering only).

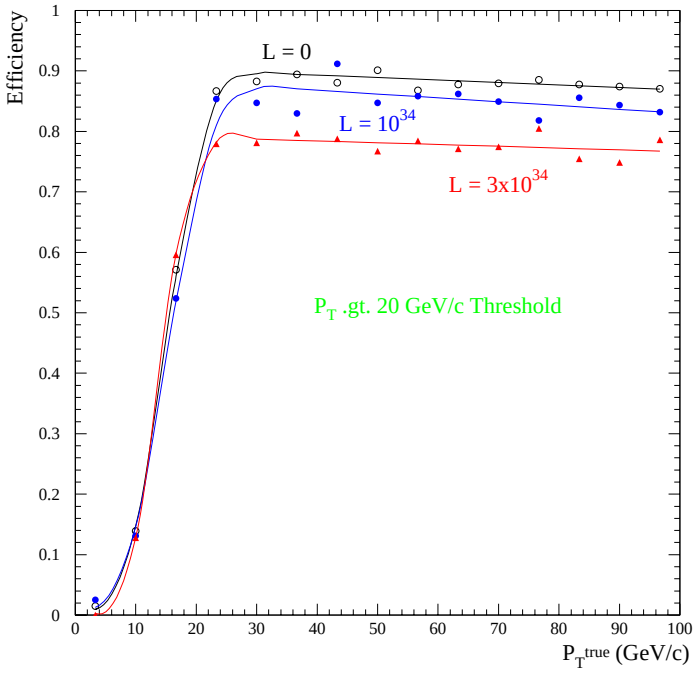

Figure 11: CSC trigger efficiency as a function of p_{T} for a threshold of 20 GeV/c. Pile-up from minimum-bias collisions and neutrons are added for luminosities of 0, 10^{34}, and 3×10^{34} cm^{-2} s^{-1}.

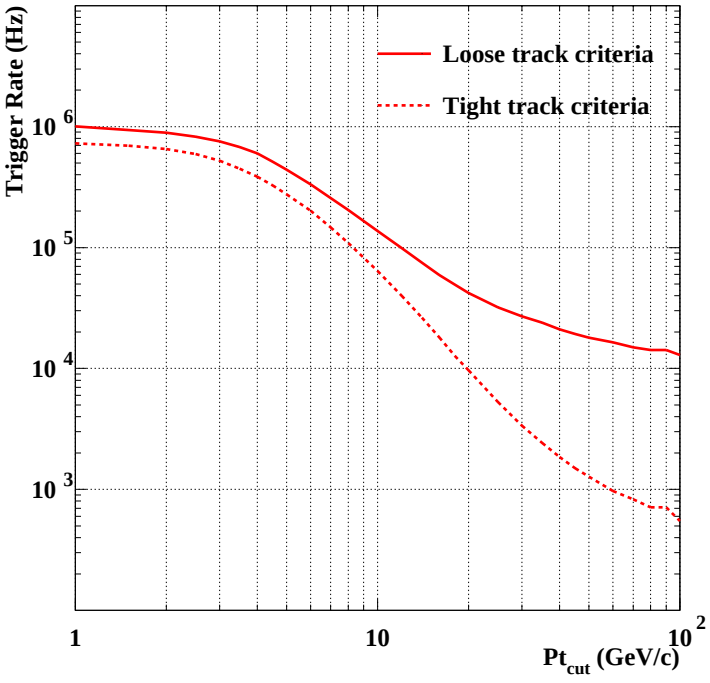

Figure 12: Single muon trigger rate from the CSC Track-Finder as a function of the p_{T} threshold (defined at 90% efficiency) for a luminosity of 10^{34} cm^{-2}s^{-1}. Estimate is based on ORCA_4_3_2 and weighted minimum bias events. The solid line corresponds to loose requirements on the track quality, the dashed line corresponds to tight requirements.

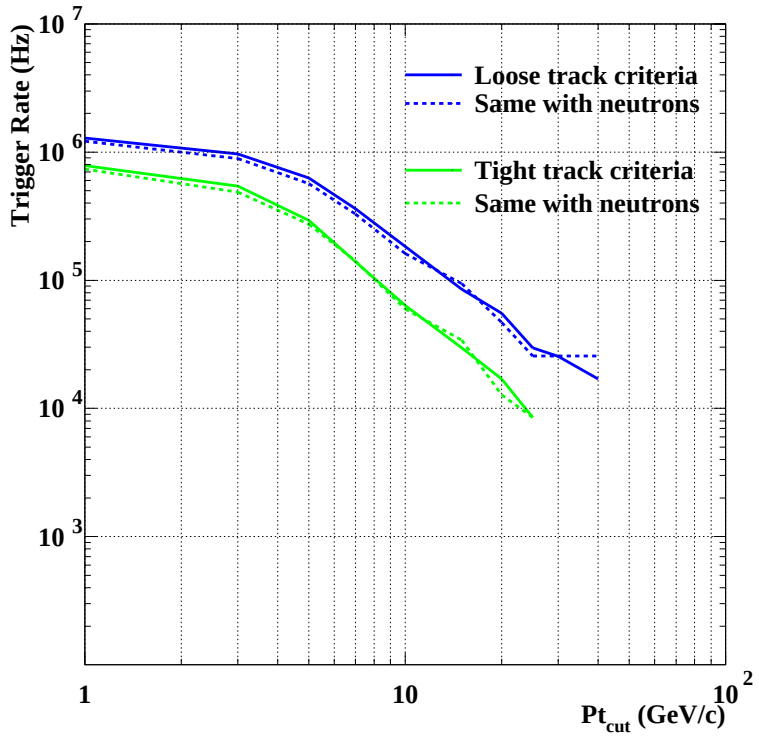

Figure 13: New estimate of the single muon trigger rate from the CSC Track-Finder as a function of the p_{T} threshold based on ORCA_4_5_1 and unweighted minimum bias events. Solid lines denote the rate for a luminosity of 10^{34} cm^{-2}s^{-1} without the effects of pile-up. Dashed lines denote the rate when pile-up effects and the neutron background are included. The upper two curves correspond to loose requirements on the track quality, while the lower two curves correspond to tight requirements.

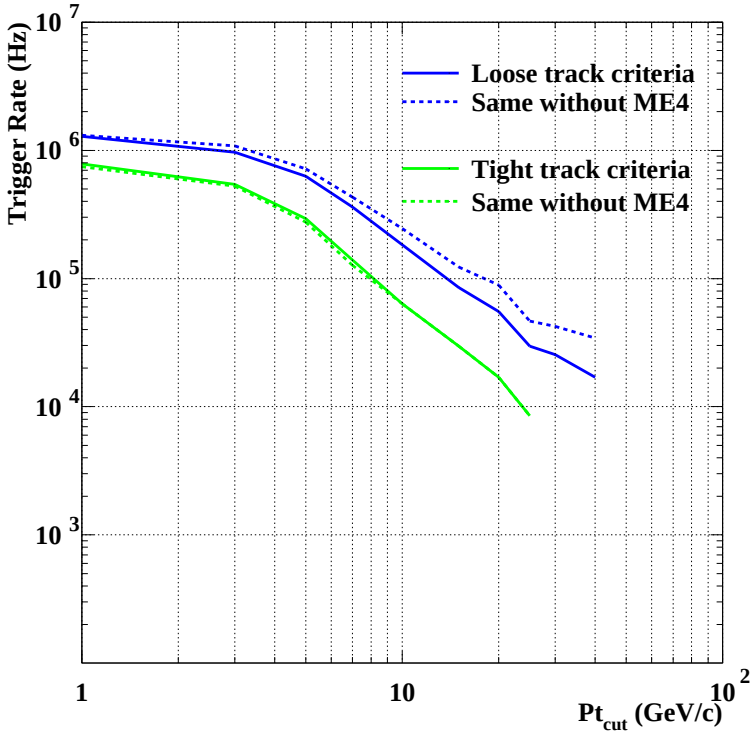

Figure 14: Single muon trigger rate from the CSC Track-Finder as a function of the p_{T} threshold with and without ME4 included.

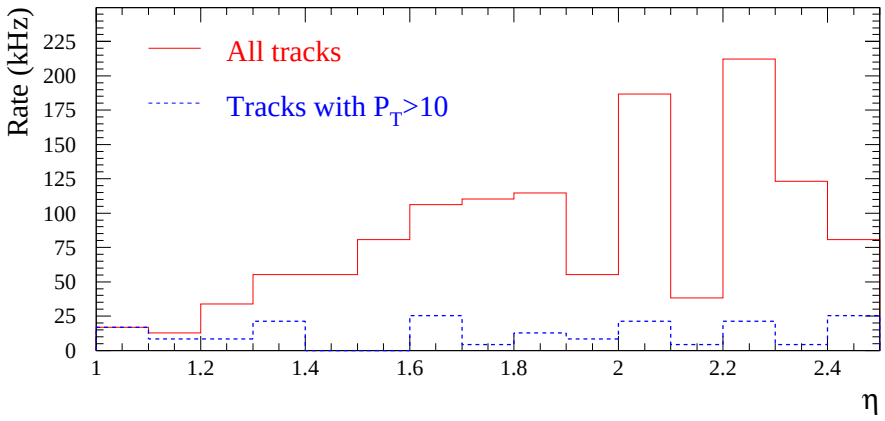

Figure 15: Single muon trigger rate from the CSC Track-Finder as a function of the η for two p_{T} thresholds: 0 and 10 GeV/c.